FULLY-REVERSED CYCLIC FATIGUE OF A WOVEN CERAMIC MATRIX COMPOSITE AT ELEVATED TEMPERATURES

Mehran Elahi, Elizabeth City State University

Abstract

Ceramic matrix composites provide characteristics suitable for high-temperature applications such as jet engines, due to their high strength and toughness, low density, creep and thermal shock resistance. The use of continuous fiber-reinforced ceramic-matrix composites for propulsion applications requires evaluation of performance and durability of these materials under static and cyclic loading at elevated temperatures. This paper presents the results of an experimental study as part of a larger investigation, to characterize cyclic fatigue response of a SiC/SiC composite-material system. In this study, the author investigated and characterized the behavior of fiber-reinforced silicon-carbide matrix composites at 1800 °F under fully-reversed cyclic loading with a frequency of 1 Hz. Results for various stress levels representing various states of damage are presented. Results of tests for cross-ply and quasi-isotropic laminates are presented and compared.

Introduction

Reinforcement of ceramic materials with high modulus and high strength fibers has resulted in tougher materials with improved properties such as strength, fracture resistance [1], fatigue resistance, creep resistance and thermal shock resistance [2]-[3]. These improved properties prompted many researchers to look into potential uses of these materials in structures with launch technology propulsion applications [4], nuclear applications [5], or as fasteners [6], among others. For propulsion applications, with operating temperatures well above 1800 °F, evaluation of performance and durability of any candidate material under static and cyclic fatigue loading is required. This study followed the previous work by the author and is intended to characterize the thermo-mechanical behavior of a model material, silicon-carbide fiber (Nicalon) reinforced enhanced silicon-carbide matrix composite (Nicalon[1]/E-SiC) processed by a chemical vapor infiltration technique (CVI) [7].

.

Investigative Approach

The emphasis was mainly on the cyclic fatigue behavior of this material at elevated temperatures.

Potential damage modes and failure mechanisms as a function of applied load levels—stacking sequence, specimen geometry, and test temperature—are discussed. This study was part of a larger investigation and followed the earlier experimental research [7]. In the near future, the results of this study will be used for calibration of a prediction model, which is based on a damage-accumulation concept and uses remaining strength as a damage metric, to predict life and remaining strength

Fully-reversed cyclic loads are considered by many to be the most damaging to fiber composites because of activation of both tensile and compressive damage modes. Depending on the relative competition of these damage modes, either tensile or compressive-failure will be the controlling mode. Therefore, fully-reversed loading provides an opportunity to observe different damage mechanisms in composite laminates. In a load-controlled mode, bow-tie shaped specimens with stacking sequences of $[(0,90)/(0,90)]_{2s}$ (cross-ply) and $[(0,90)/(+45,-45)]_{2s}$ (quasi-isotropic) were subjected to a sinusoidal waveform with a frequency of 1 Hz, and a fatigue ratio of R=-1 under atmospheric air at 1800 °F (Figure 1).

Figure 1. Geometry of test specimens

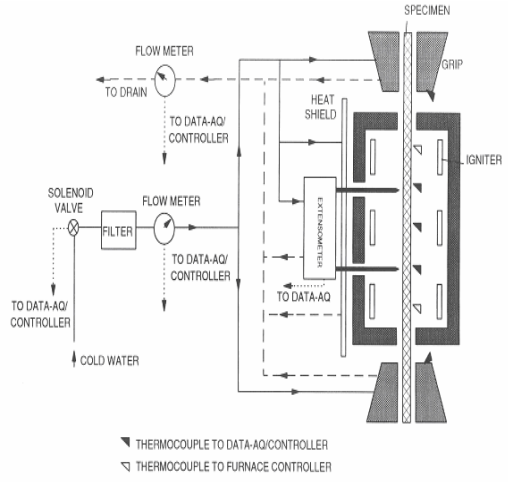

Figure 2. Schematic of the test set-up for elevated-temperature axial testing

The proposed test matrix for cross-ply and quasi-isotropic laminates is presented in Table 1. Based on the availability of specimens at least two specimens were tested at each stress level. A run-out (RO) test, according to the High-Speed Civil Transport (HSCT) standards for cyclic fatigue of ceramic matrix composites [8], was set at 10^5 cycles. The remaining material properties of run-out specimens were obtained by conducting quasi-static tensile tests at temperatures under stroke control.

Table 1. Test matrix for cyclic tests of $[(0,90)/(0,90)]_{2s}$ and $[(0,90)/(+45,-45)]_{2s}$ laminates for R=-1, f=1 Hz, T=1800 °F

# of Specimens	Loading Mode	Max. Stress Level	% Life Cycled
2	Load	σ_1	100
2	Load	σ_2	100
2	Load	σ_3	100

Material and Specimen Geometry

Test specimens were fabricated of 2-D woven flat coupons made of Ni/E-SiC composite material. This material was processed by an isothermal chemical vapor infiltration technique (ICVI) manufactured by Du Pont Lanxide Composites, Inc. The reinforcement phase was ceramic grade Nicalon fiber (0/90 plain weave cloth) and the matrix material was enhanced SiC (containing boron-based particles for protection of fibers against oxidation). Each ply had a thickness of 0.0105″, a density of 0.83 lbs/in^3, a fiber volume fraction of 40%, and a porosity of 12%. Specimens were cut from 12″×12″ panels with cross-ply and quasi-isotropic stacking sequences into bow-tie shapes using a water-jet technique. Based on their width, specimens were categorized as wide specimens (average thickness = 0.09″, gage section width = 0.75″, grip section width = 0.85″, and length = 6.0″), and the narrow specimens (thickness = 0.09″, gage section width = 0.40”, grip section width = 0.50″, and length = 6.0″). Finally, for protection against oxidation, a layer of SiC (80-100 μm) was deposited on the outer surface.

Utilizing an elevated-temperature axial testing system (Figure 2) and tensile test results of cross-ply and quasi-isotropic laminates at 1800 °F obtained from the first phase of this investigation [7], fully-reversed cyclic fatigue tests were carried out at 1800 °F under three different stress levels. According to the tensile stress-strain curve for these laminates (Figures 3 & 4), these stresses correspond to locations of well below, right at, and well above the Proportional Limit Strength (PLS). Based on a PLS of 12.7 ksi (measured using a 0.005% offset strain method), stresses of σ_1=10 ksi, σ_2=13 ksi, and σ_3=15 ksi were chosen as the maximum applied stress levels. The 10 ksi stress level is located within the linear elastic range; the 13 ksi stress level is located in a region where material is going through the transition from linear elastic regime to nonlinear regime; and, the 15 ksi stress level is located in a nonlinear regime past the transition region.

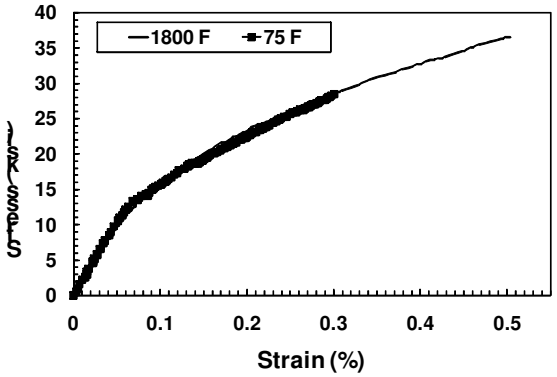

Figure 3. Room and elevated temperature tensile responses of [(0,90)/(0,90)]2s laminates

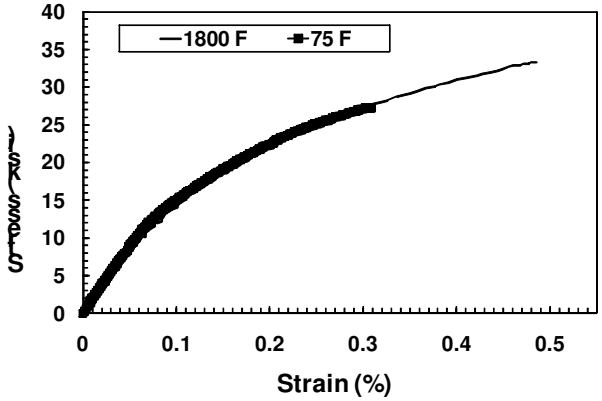

Figure 4. Room and elevated temperature tensile responses of [(0,90)/(+45,-45)]2s laminates

Cross-Ply Laminates

From a total of seven specimens designated for this testing category, two were tested at 10 ksi, two at 13 ksi and three at 15 ksi stress levels. At least one 0.75″-width specimen was included in each stress level. All of the 10 ksi tests lasted more than 10^5 cycles (representing an exposure time of 28 hours at temperature) and were considered as run-outs. Typical stress-strain loops were collected using an x-y plotter (Figure 5). Close inspection reveals that the application of the first loading cycle resulted in a small amount of hysteresis on the tensile-loading side of the curve, which lasted almost $5x10^4$ cycles and gradually disappeared upon further cycling. This energy dissipation is believed to be associated with the presence of matrix micro-cracks at this load level. Damage mechanisms such as stretching of fibers, breaking of fibers, sliding of interfaces, and crack deflection can also

contribute, either alone or in combination, to energy dissipation. The small magnitude of hysteresis area at this load level did not permit an accurate measurement although stiffness measurements were made. During these tests, damage and damage evolution were confined to the tensile side of loading. This was expected as the Ultimate Compression Strength (UCS) for this material is reported to be almost twice as large as the Ultimate Tensile Strength UTS [9].

Tensile tests under stroke control at 1800 °F were conducted on the run-out specimens. Large scatters in initial elastic modulus values (Young's elastic modulus prior to cycling) were present, which might have contributed to variation in material response (especially in strain to failure). The scatter in initial elastic modulus values was believed to be directly related to the degree of porosity for these material systems. A nominal value ranging from 10% to 12% has been reported. In the initial elastic region, matrix contributes substantially to the modulus of composite. Presence of any porosity results in lower actual matrix volume fraction, thereby causing a reduction in the elastic modulus. This may explain why there is larger scatter in elastic modulus than tensile strength.

The 10 ksi tests did not result in failure of specimens. Initial elastic modulus, representing the virgin state of material, was measured and recorded. Measured remaining properties indicated an average final elastic modulus (Young's elastic modulus after cycling) of 16.13 Msi, a remaining strength (Sr) of 26.16 ksi, and a remaining strain-to-failure of 0.278% (Table 2). These values represented a decrease of 7%, 27%, and 47% from the corresponding average values obtained from the tensile test of virgin specimens at 1800 °F. Due to the presence of large scatter in initial elastic modulus, the percent reduction in modulus was based on the average initial elastic modulus of the same (17.38 Msi in case of the 10 ksi test) specimens, which is much smaller than 20.50 Msi reported previously). The PLS and its associated strain remained basically unchanged. Specimens with wider gage width provided higher remaining properties.

The 13 ksi tests resulted in failure of all specimens, where an average life of 26,000 cycles was recorded (representing an exposure time of 8 hours). Typical stress-strain loops were collected and results are presented in Figure 6. The stress-strain hysteresis loops indicated significant amounts of damage, generated upon application of the first loading cycle. This was expected as the 13 ksi stress level caused significant matrix cracking. An average value of 18.37 Msi was obtained for initial elastic modulus. Similar to 10 ksi tests, damage initiated on the tensile side of loading. Upon further cycling, damage evolved and grew slowly into the compression side. The presence of a small amount of hysteresis on the compression side may, in part, be explained by the fact that the 13 ksi stress level was large enough to produce fiber matrix de-bonding, matrix crack, fiber fracture, and fiber pull-out. Depending on the position of broken fibers and the large matrix cracks upon unloading, some of these broken fibers did not go back into the matrix from which they were pulled. The ends of the broken fibers were deflected such that they prevented full crack closure.

This argument was supported by the absence of stiffness degradation on the compression side of stress-strain curves, where the unloading compressive modulus provided the same value as loading compressive modulus. The hysteresis area increased steadily from the second cycle with the highest hysteresis occurring on the last cycle before final failure. It was not possible to capture the last few cycles before final failure without running the risk of computer storage overflow. The specimen with larger gage width lasted longer.

Depending on the gage width, the 15 ksi tests showed large scatter in cycles to failure values. The wider specimens lasted almost twice as long as the narrow specimens. Narrow specimens showed similar cycles to failure averaging at 12,350 cycles (representing an exposure time of almost 3.75 hours). It was decided to discard the life of the wide specimens and use the average life of narrow specimens as the reference life. This life is almost half of the life for 13 ksi tests. The measured initial elastic modulus values were very close, averaging 18.03 Msi. Typical hysteresis loops were collected and are presented in Figure 7. As is indicated by the size of the hysteresis loops, 15 ksi stress levels generated more damage in the material than the other two stress levels. Similarly, damage was initially confined to the tensile loading side (at least for the first 100 cycles).

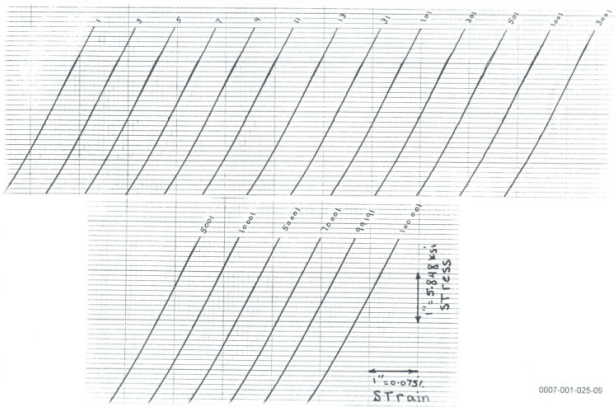

Figure 5. Stress-strain loops for a [(0,90)/(0,90)]2s laminate for σ_{max}=10 ksi, R=-1, and f=1 Hz at 1800 ºF

Upon further cycling, hysteresis grew into the compression side. As to the nature of hysteresis on the compression side, the same argument as for the 13 ksi tests may be applied

here. It should be noted that in all of these tests, tensile failure proved to be the dominant failure mode and always occurred in the specimen's discoloration zone.

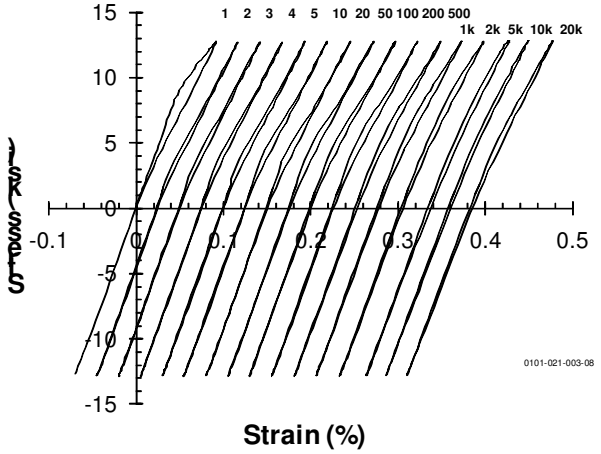

Figure 6. Stress-strain loops for a [(0,90)/(0,90)]2s laminate for σ_{max}=13 ksi, R=-1, and f=1 Hz at 1800 ºF

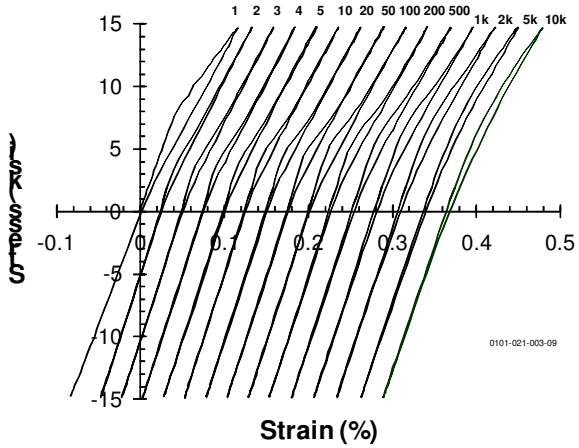

Figure 7. Stress-strain loops for a [(0,90)/(0,90)]2s laminate for σ_{max}=15 ksi, R=-1, and f=1 Hz at 1800 ºF

Normalizing the applied stresses with respect to UTS, the S-N diagram (stress-cycle relationship), when plotted with a semi-log axis, indicates a straight line (Figure 8). This line may best be represented by (Sa/Su) = 1.0008-0.0624*Log (N), where Sa, Su, and N represent the applied stress, ultimate tensile strength, and number of loading cycles, respectively. These results indicate that matrix cracking played the most important role. With stress levels at or above the PLS, the composite has a short life. Also, porosity seemed to influence the fatigue response. This assessment was supported by the presence of large amounts of porosity at the fractured surfaces. Moschelle et al. [10] have reported similar observations based on room-temperature fatigue test results of regular Nicalon/SiC.

Table 2. Fatigue test results of $[(0,90)/(0,90)]_{2s}$ laminates for R=-1, and f=1 Hz, at 1800 ºF

Spec.I. D. & Width	σ_{max} (ksi) & Cycles	Ei & Ef (Msi)	PLS (ksi) & Strain (%)	Sr (ksi) & Strain (%)
025-09 (0.40″)	10.0 RO, OX	16.41 & 14.99	11.70 & 0.075	24.85 & 0.263
020-09 (0.75″)	10.0 RO, IX	18.34 & 17.26	13.59 & 0.079	27.51 & 0.293
Ave. Value	**10.0 RO**	**17.38 & 16.13**	**12.65 & 0.077**	**26.18 & 0.278**
024-07 (0.40″)	13.0, OX 23515	18.10 & NA	NA	NA
020-08 (0.75″)	13.0, OX 28486	18.63 & NA	NA	NA
Ave. Value	**13.0 26000**	**18.37 & NA**	**NA**	**NA**
021-08 (0.40″)	15.0, OX 12679	18.12 & NA	NA	NA
023-10 (0.40″)	15.0, OX 12022	17.93 & NA	NA	NA
018-10 (0.75″)	15.0, IX 21825	NA	NA	NA
Ave. Value	**15.0 12350**	**18.03**	NA	NA

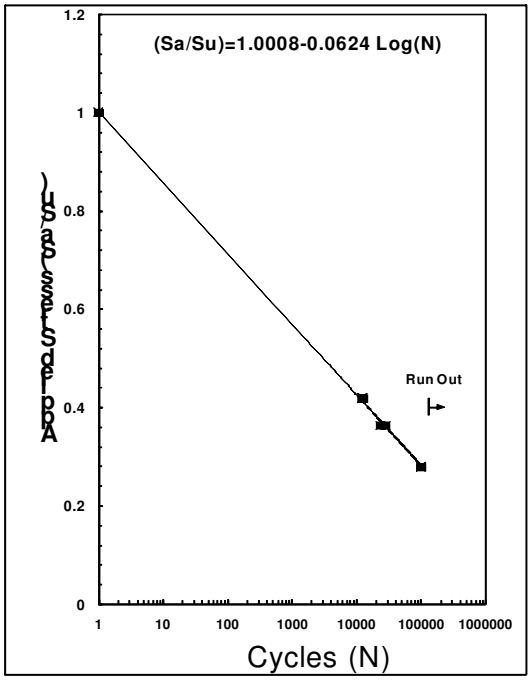

Figure 8. Cyclic fatigue response of [(0,90)/(45,-45)]2s laminates for R=-1, and f=1 Hz at 1800 ºF

Quasi-Isotropic Laminates

Similar to cross-ply laminates, all of the 10 ksi tests resulted in run-outs. The stress-strain loops indicated similar

characteristics as the cross-ply laminates (Figure 9) with an average initial elastic modulus of 17.76 Msi. Based on quasi-static tensile tests at 1800 °F, an average final elastic modulus of 16.35 Msi, a remaining strength of 25.56 ksi, and a remaining strain to failure of 0.289% were recorded (Figure 12).

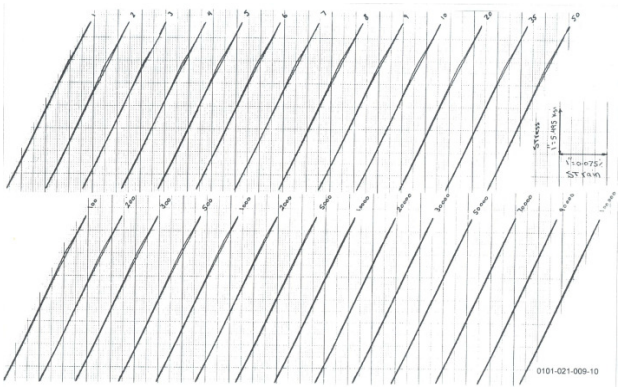

Figure 9. Stress-strain loops for a [(0,90)/(45,-45)]2s laminate for σ_{max}=10 ksi, R=-1, and f=1 Hz at 1800 °F

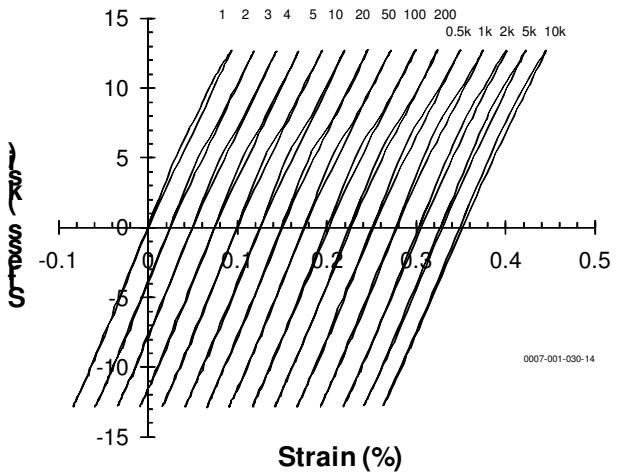

Figure 10. Stress-strain loops for a [(0, 90)/(45,-45)]2s laminate for σ_{max}=13 ksi, R=-1, and f=1 Hz at 1800 °F

The 13 ksi tests resulted in an average life of 25,140 cycles (an exposure time of 7.25 hours). This is very similar to the average life of cross-ply laminates. An average initial elastic modulus of 18.26 Msi was obtained. The typical stress-strain loops are presented in Figure 10. The evolution of hysteresis resembled those of cross-ply specimens and the same argument for the presence of hysteresis may be applied. The 15-ksi stress-level tests resulted in an average life of 14,800 cycles (an exposure time of 4.36 hours). Similar to cross-ply laminates, this life was almost half of the life achieved by 13 ksi tests. Unlike 13 ksi tests, the life for 15 ksi tests was slightly higher than its cross-ply counterpart. An average value of 16.97 Msi was recorded. Typical stress-strain hysteresis loops are shown in Figure 11.

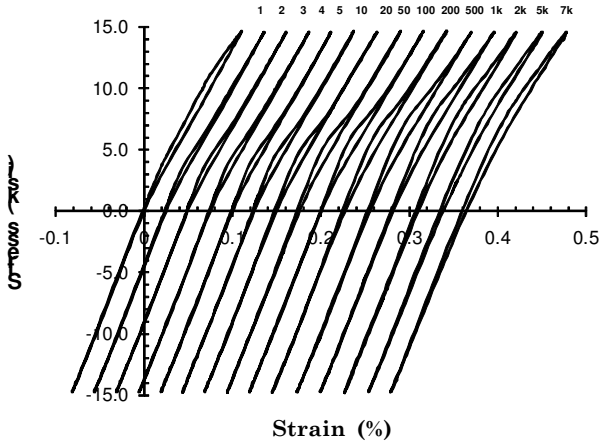

Figure 11. Stress-strain loops for a [(0,90)/(45,-45)]2s laminate for σ_{max}=15 ksi, R=-1, and f=1 Hz at 1800 °F

Spec.I .D. & Width	σ_{max} (ksi) & Cycles	Ei & Ef (Msi)	PLS (ksi) & Strain (%)	Sr (ksi) & Strain (%)
009-09 (0.40)	10.0 RO, IX	18.63 & 16.82	12.36 & 0.077	26.38 & 0.300
009-10 (0.40)	10.0 RO, IX	16.89 & 15.87	12.36 & 0.082	24.73 & 0.277
Ave. Value	**10.0 RO**	**17.76 & 16.35**	**12.36 & 0.079**	**25.56 & 0.289**
030-01 (0.40)	13.0, OX 24300	18.01 & NA	NA	NA
030-02 (0.40)	13.0, OX 25980	18.51 & NA	NA	NA
Ave. Value	**13.0 25140**	**18.26 & NA**	**NA**	**NA**
030-03 (0.40)	15.0, OX 15614	17.56 & NA	NA	NA
030-04 (0.40)	15.0, OX 13986	16.37 & NA	NA	NA
Ave. Value	**15.0 14800**	**16.97 &NA**	**NA**	**NA**

Figure 12. Fatigue test results for [(0,90)/(+45,-45)]$_{2s}$ laminates with R=-1, and f=1 Hz, at 1800 °F

In general, the off-axis lamination did not significantly influence the fatigue response. The S-N diagram showed characteristics similar to the cross-ply laminates. The fatigue S-N data may best be represented by a straight line such as

(Sa/Su) = +1.0032-0.0595 Log (N), as shown in Figure 13. The slope of this line was slightly lower than the one for the cross-ply case. Comparison of average remaining properties of cycled specimens with the corresponding un-cycled values indicated a reduction of 8%, 23% and 37% in elastic

modulus, UTS and strain to failure, respectively. With an offset strain of 0.005% and a PLS of 12.36 ksi, with a corresponding strain of 0.079%, were also obtained. A comparison between remaining strength and remaining strain values of cross-ply and quasi-isotropic laminates did not show significant differences in property degradation as a function of stacking sequence (Figure 14).

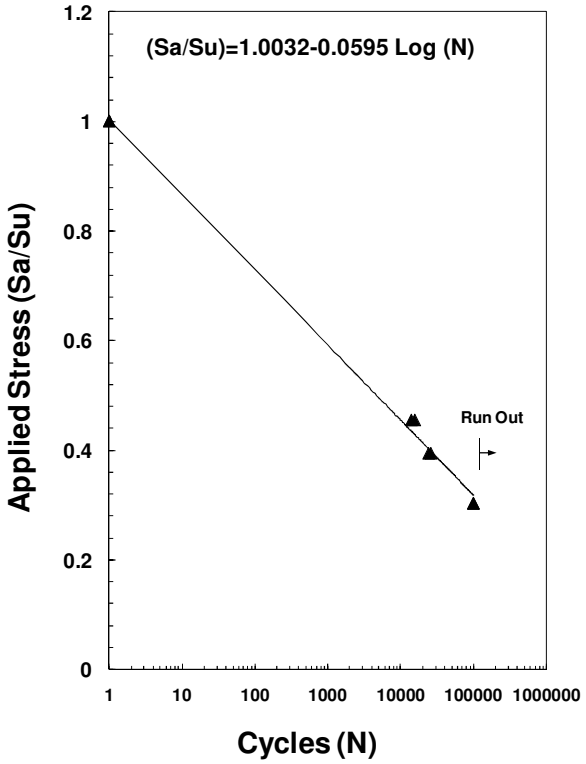

Figure 13. Cyclic fatigue response of [(0,90)/(45,-45)]2s laminates for R=-1, and f=1 Hz at 1800 ºF

Summary

In fully-reversed cyclic fatigue tests, the compression part of loading, in general, does not influence the material response directly, but reduces the time that cracks stay open by half. Cross-ply and quasi-isotropic laminates show very similar fatigue behavior, remaining strength, and life. Results indicate that matrix cracking plays the most important role. With stress levels at or above the proportional limit strength, the composite has a short life. Also, porosity seems to influence the fatigue response significantly. This assessment was supported by the presence of a large amount of porosity at the fractured surfaces. The fatigue threshold stress, the level at which run-out occurs, is believed to be lower than the proportional limit strength.

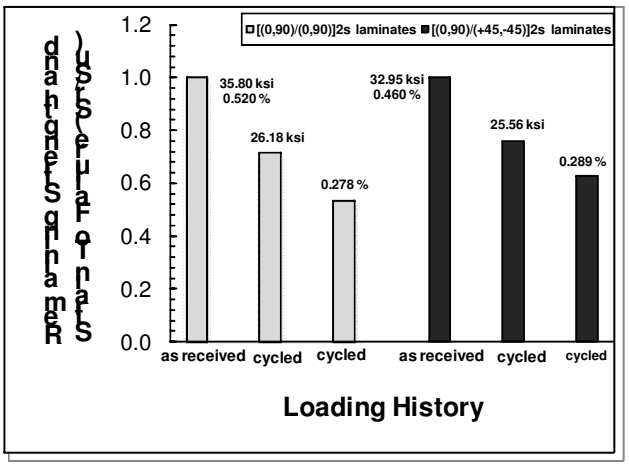

Figure 14. Remaining strength and strain for [(0,90)/(0,90)]2s and [(0,90)/(+45/-45)]2s laminates after 100k cycles, σmax=10 ksi, R=-1, and f=1 Hz at 1800 °F

Further Research

To have a better picture of the fatigue response for these materials, more tests are needed to complete the S-N diagram. The next phase of this research will also include indentifying damage modes and failure mechanisms and to quantify damage accumulation in terms of stiffness degradation and remaining strength. The intention is to use the results of this study to enable and calibrate a prediction model. This model, which is based on a damage-accumulation concept and uses remaining strength as a measure of damage, will be utilized to predict life and remaining strength.

References

[1] E.L. Courtright, H.C. Graham, A.P. Katz, and R.J. Kerans, "Ultra High Temperature Assessment Study-Ceramic Matrix Composites," NASA Technical Report WL-TR-91-4061, Sep. 1992.

[2] K.K. Chawla, "Composite Materials Science and Engineering" New York:Springer-Verlag, Inc., 1987, page 250.

[3] L.C. Sawyer, M. Jamieson, D. Brikowski, M.I. Haider, and R.T. Chen, "Strength,Structure, and Fracture properties of Ceramic Fibers Produced from Polymeric Precursors: I, Base-Line Studies," J.Am.Ceram.Soc., 70 [11] 798-810 (1987).

[4] Kiser, J.D., et al.: Durable High Temperature Ceramic Matrix Composites for Next Generation Launch Technology Propulsion Applications. Proceedings of the JANNAF 27th Airbreathing Propulsion Subcommittee Meeting, CPIA-JSC-CD-24, 2003. Available from Chemical Propulsion Information Agency (CPIA).

[5] W. E. Windes, P. A. Lessing, Y. Katoh, L. L. Snead, E. Lara-Curzio, J. Klett, C. Henager, Jr., R. J. Shinavski, "Structural Ceramic Composites for Nuclear Applications, " Technical report, Idaho National Laboratory, INL/EXT-05-00652, Aug. 2005.

[6] M.J. Verrilli, D. Brewer, "Characterization of Ceramic Matrix Composite Fasteners Exposed in a Combustion Liner Rig Test" Proceedings of ASME/IGTI TURBO EXPO 2002, June 3-6, Amsterdam, Netherlands.

[7] M. Elahi, "Characterization of Tensile Properties of Woven Ceramic Composites at Room and Elevated Temperature," Proceedings of The 2008 IAJC-IJME International Conference, ISBN 978-1-60643-379-9.

[8] Tension-Tension Load Controlled Fatigue Testing of Ceramic Matrix, Intermetalic Matrix and Metal Matrix Composite Materials, HSR/EPM-D-002-93 Consensus Standard, GE Aircraft Engines, 1 Neumann Way, Mail Drop G-50, Cincinnati, OH. 45215-6301.

[9] M.H. Headinger, D.H. Roach, and D.J. Landini, "High Temperature Fatigue of Ceramic Matrix Composites," Presented at AeroMat 1994.

[10] W.R. Moschelle, "Load Ratio Effects on the Fatigue Behavior of Silicon Carbide Fiber Reinforced Silicon Carbide," Ceram.Eng.Sci.Proc., Vol 15, [4], 1994, 13-22.

Biographies

MEHRAN ELAHI is an associate professor in the Department of Technology at Elizabeth City State University. He received his B.S. and M.S. degrees in Mechanical Engineering from Mississippi State University, Starkville, MS, in 1992, and 1995, respectively. He received a Ph.D. from the Engineering Science and Mechanics Department at Virginia Tech, Blacksburg, VA, in 1996. His areas of interest are solid mechanics, composite materials, material characterization, fatigue and creep of engineering materials. Dr. Elahi may be reached at melahi@mail.ecsu.edu